

Catalytic activity of aminopropyl xerogels in the selective synthesis of (*E*)-nitrostyrenes from nitroalkanes and aromatic aldehydes

G. Sartori,^{a,*} F. Bigi,^a R. Maggi,^a R. Sartorio,^a D.J. Macquarrie,^b M. Lenarda,^c L. Storaro,^c S. Coluccia,^d and G. Martra^d

^a “Clean Synthetic Methodologies Group,” Dipartimento di Chimica Organica e Industriale dell’Università, Parco Area delle Scienze 17A, I-43100 Parma, Italy

^b Department of Chemistry, University of York, Heslington, York, YO10 5DD, UK

^c INSTM UdR di Venezia, Dipartimento di Chimica, Università di Cà Foscari, Via Torino 155/b, I-30174 Mestre Venezia, Italy

^d Dipartimento di Chimica IFM dell’Università, Via Pietro Giuria 7, I-10125 Turin, Italy

Received 3 September 2003; revised 21 November 2003; accepted 24 November 2003

Abstract

Various aminopropyl-functionalized silicas (APS) were prepared by the sol–gel technique using different tetraethyl orthosilicate/aminopropyltriethoxysilane (TEOS/ATS) ratios and tested as base catalysts for the nitroaldol reaction. The solids were fully characterized. It was proved that the amount of organic component strongly influences the composition and textural properties of the hybrid organic–inorganic materials. In particular, when ATS was increased to more than 40%, pore volume collapse was observed and a significant decrease in interaction with benzaldehyde reagent was revealed by FT-IR. Catalytic activity in the nitroaldol reaction was correlated with chemical composition and textural properties, suggesting that the catalyst efficiency depends on accessibility to the catalytic sites. In all cases, (*E*)-nitrostyrene was selectively obtained.

© 2003 Elsevier Inc. All rights reserved.

Keywords: Aminopropyl silica; Base catalyst; Nitroaldol condensation; Nitroalkene; Hybrid organic–inorganic material; Infrared

1. Introduction

Preparation of fine chemicals and pharmaceuticals has been recognized as the sector of industrial chemistry most responsible for production of waste defined as “*everything produced in the overall process but the desired product*” [1]. Cleaner technologies are required by increasingly stringent environmental regulations. Accordingly, the chemical industry is rethinking its strategies.

As expected, reducing emissions and waste results in an improvement of the production process from both environmental and economical points of view. Use of heterogeneous catalysts, which are more stable and easier to remove and reuse, can improve overall liquid-phase synthetic methodology and product quality [2,3].

The nitroaldol reaction represents an important carbon–carbon forming process by which variously functionalized

nitro compounds can be synthesized via condensation of nitroalkanes with carbonyl compounds in the presence of basic catalysts. Different organic and inorganic base catalysts have been used including primary and tertiary amines and alkali metal hydroxides, carbonates, and alkoxides [4–6]. This reaction is frequently accompanied by unwanted side reactions such as the Cannizzaro reaction of carbonyl compounds and the Michael addition or polymerization when nitroalkenes are produced. These side reactions can be minimized or completely avoided by careful control of the basicity of the catalyst.

Our interest in the preparation and use of solid catalysts for production of fine chemicals [7–10] prompted us to deeply investigate nitroalkene synthesis via nitroaldol condensation of nitroalkanes and aldehydes in the presence of different solid bases composed of propylamine anchored to siliceous supports [11].

Several articles have recently reported the use of Mg–Al hydrotalcites [12] or amino [13]- and diamino [14]-functionalized mesoporous materials as heterogeneous catalysts for

* Corresponding author.

E-mail address: giovanni.sartori@unipr.it (G. Sartori).

the nitroaldol reaction. The catalysts reported in the present study were prepared by sol–gel processes from mixtures of tetraethoxysilane (TEOS) and aminopropyltriethoxysilane (ATS). The great advantage of this technique is the mild conditions required. In particular, the synthesis performed at low temperature allows the incorporation of organic functions, including chiral moieties, into the inorganic framework [15, 16]. With such a methodology, materials with unique physical and chemical properties can be prepared by an appropriate combination of inorganic and organic reagents.

The efficiency of aminopropylsilica heterogeneous catalysts (APS) prepared by gelation of different mixtures of TEOS and ATS in the model nitroaldol condensation between nitromethane and benzaldehyde was studied and related to the physicochemical parameters of the catalysts.

2. Experimental

2.1. Materials

All materials purchased were used as such. Starting materials for catalyst preparation: tetraethyl orthosilicate (> 98%, Aldrich), (3-aminopropyl)triethoxysilane (> 98%, Fluka). Starting materials for nitroaldol condensation: benzaldehyde (> 99%, Fluka), *p*-anisaldehyde (> 98%, Fluka), *p*-hydroxybenzaldehyde (> 98%, Fluka), *p*-chlorobenzaldehyde (> 98%, Fluka), *p*-nitrobenzaldehyde (> 99%, Fluka), nitromethane (> 99%, Fluka), nitroethane (> 97%, Fluka).

2.2. Catalyst preparation

APS were prepared as follows: In a beaker containing methanol, TEOS, and the selected amount of ATS (for reagent amounts see Table 1), the water required for the hydrolysis (equimolecular with respect to the alkoxy groups) is added dropwise with vigorous stirring at room temperature. When the mixture begins to become opalescent, the stirrer is stopped and the formed gel is aged for 20 days at room temperature in the same container covered with filter paper. The white monolith so obtained is then finely ground in a mortar. Then 10 g of powder is washed on a Büchner funnel with water (500 mL), methanol (200 mL), ethyl acetate (200 mL), diethyl ether (200 mL) and hexane (200 mL). The material

is heated in an oven at 110 °C for 2 h and finally sieved to 80–120 mesh.

2.3. Catalyst characterization

All materials were characterized with respect to compositional, textural, and surface properties.

The loading of the aminopropyl groups was calculated from the nitrogen content by elemental analysis performed with a Carlo Erba CHNS-0 EA1108 Elemental Analyzer.

Thermogravimetric analysis revealed that all these materials are thermally stable and they do not lose organic fragments until 350 °C.

N₂ adsorption–desorption isotherms, obtained at –196 °C on a Micromeritics ASAP 2010, were used to determine specific surface areas, *S*_{BET}. Before each measurement the samples were outgassed at 110 °C and 1.33 × 10^{–4} Pa for 12 h.

Pore volume was calculated by the classic Kelvin equation using cylindrical pore geometry and the Broekhoff–de Boer model [17].

IR spectroscopy was employed for the investigation of structural and surface properties; in this last case also the adsorption of benzaldehyde was monitored by this technique. For IR measurements, the sample, in the form of a self-supporting pellet, was placed into a conventional quartz cell, equipped with KBr windows, which was permanently connected to a vacuum line (residual pressure: 1.33 × 10^{–4} Pa). The outgassing of the sample and the adsorption and desorption of benzaldehyde were then carried out in situ, at room temperature. IR spectra were recorded with a Bruker Vector 22 at 4 cm^{–1} resolution.

To correctly compare the intensities of the spectra of the various samples independently of their masses, for each sample the spectral intensity for unit mass (mg) has been reported.

For the adsorption experiments, benzaldehyde from Sigma–Aldrich (reagent grade) was used, after several freeze–pump–thaw cycles.

2.4. Reaction procedure for nitroaldol condensation

Nitroaldol condensation of benzaldehyde and nitromethane as model reagents was performed using a batch-type reactor. The experimental conditions were as follows: A mixture of benzaldehyde (5.0 mmol, 0.53 g, 0.51 mL), nitromethane (6 mL), and the selected catalyst (the amount of which was selected on the basis of loading value in order to introduce the same amount of propylamine in all experiments, maintaining the molar ratio of benzaldehyde/propylamine at 40.0) was kept at 90 °C under magnetic stirring for 2 h. The mixture was then cooled to room temperature and filtered on Büchner funnel. The solid catalyst was washed with acetone, methylene chloride, and ethyl acetate (10 mL each) and the solution so obtained was analyzed by GC [fused silica capillary column SPB-1 (30 m × 0.25 mm) was used with helium

Table 1
Synthesis of APS

Material	TEOS (mmol)	ATS (mmol)	H ₂ O (mmol)	Methanol (mL)
APS10	72	8	312	29
APS20	56	14	266	20
APS30	47	20	248	31
APS40	39	26	234	33
APS50	40	40	280	45
APS60	39	51	309	51

as carrier on a DANI 8221 instrument connected to a HP 3396 A integrator].

The same methodology was used in the synthetic application to different aldehydes and nitroalkanes by using the best catalyst, APS-40. The products were purified by flash chromatography over silica gel column, using hexane–ethyl acetate mixtures as eluants. All products gave melting points and spectral data consistent with those reported.

3. Results and discussion

3.1. Catalyst characterization

3.1.1. Porosity and surface area

The sample codes and basic physical characteristics are listed in Table 2. N_2 adsorption isotherms are commonly used in organic–inorganic nanocomposite materials, allowing determination of specific surface area, pore volume, and pore size distribution. The N_2 adsorption isotherms of APS catalysts exhibit a profile corresponding to type II of the BDDT classification [18]. The surface area and total pore volume values follow a volcano trend (Fig. 1) that reaches higher values for samples prepared from gels with a TEOS/ATS ratio between 4 and 1.5 (mmol/mmol). A total drop in porosity was observed when the amount of ATS

Table 2
Specific surface area (SSA_{BET}) and total pore volume (V_{tot}) of APS catalysts

APS	SSA_{BET} (m^2/g)	V_{tot}^a (cm^3/g)
APS10	96.1	0.22
APS20	133.8	0.67
APS30	137.3	0.79
APS40	105.5	0.86
APS50	56.5	0.38
APS60	0.5	0.00

^a Amount adsorbed at $p/p^0 = 0.98$.

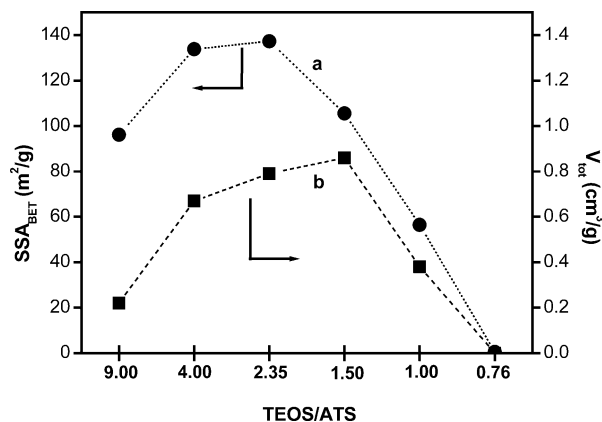


Fig. 1. Diagrams of (a) specific surface area (BET, m^2/g) and (b) total volume (cm^3/g) for the series of APS catalysts.

exceeds that of TEOS. In all cases, the pore size was disorderly distributed.

3.1.2. FT-IR measurement

3.1.2.1. IR spectra of the catalysts Figure 2 shows IR spectra of the bare SiO_2 material (curve a) and of the APS10–APS50 catalysts (curves b–f), outgassed at room temperature. Unfortunately, the APS60 catalyst exhibited some transparency to the IR light only in the range 1800–2300 cm^{-1} , precluding its use as a probe of its structure and reactivity.

In the high-frequency region, the spectrum of bare SiO_2 (Fig. 2a) exhibits a broad and complex band, with a maximum at 3490 cm^{-1} and two partly resolved components at 3610 and 3740 cm^{-1} , which are due to hydrogen-bonded, interglobular, and weakly interacting surface silanols, respectively [19]. At lower frequency, weak bands at 1990, 1875, and 1650 cm^{-1} are present, due to overtones and combination modes of the inter- and intratetrahedral fundamental vibrational modes of the siliceous framework, which absorbed completely IR radiation below 1300 cm^{-1} .

In the spectrum of the APS10 catalyst (Fig. 2b), the band at 3490 cm^{-1} is almost completely absent, and the components at 3610 and 3740 cm^{-1} appear strongly reduced in intensity. Conversely, a very broad spread in absorption over the range 3400–2200 cm^{-1} is present, from which two sets of signals emerge: one, in the range 3400–3100 cm^{-1} , and a second in the range 3000–2850 cm^{-1} . Furthermore, another series of bands is present at frequencies lower than 1750 cm^{-1} . For the sake of clarity, the latter are shown in a zoomed view in Fig. 4, are described and commented on later.

Absorptions in the range 3000–2850 cm^{-1} , are due to the asymmetric stretching of $-CH_3$ (shoulder at 2960 cm^{-1}) and $-CH_2$ (peak at 2930 cm^{-1}) groups, while their corresponding symmetric modes both contribute to the partly resolved component at 2885 cm^{-1} [20]. The presence of bands due to $-CH_3$ indicates that during preparation of the catalyst, not all the ethoxy groups present in the parent 3-amino-

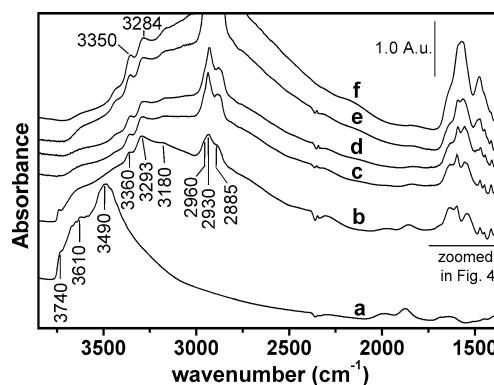


Fig. 2. IR spectra of (a) the reference SiO_2 sample and (b) APS10, (c) APS20, (d) APS30, (e) APS40, and (f) APS50 catalysts, all outgassed at room temperature for 30 min.

propyltriethoxysilane undergo hydrolysis to connect the organic substrate to the silica framework. In other words, a portion of the aminopropyl chains (R) is linked to silica by only one or two Si–O– (silica) links. However, these species should be a minority, as the intensity ratio of ν_{asym} of $-\text{CH}_3$ to ν_{asym} of $-\text{CH}_2$ appeared completely reversed with respect to that observed for the parent 3-aminopropyltriethoxysilane molecules (spectra not reported for the sake of brevity), indicating that most of the ethoxy groups were hydrolyzed.

The aminic groups of the organic chains linked to the silica framework are responsible for the absorptions at 3360 ($\nu_{\text{asym}} -\text{NH}_2$), 3293 ($\nu_{\text{sym}} -\text{NH}_2$), and 3180 cm^{-1} (first overtone of the $\delta -\text{NH}_2$ occurring at 1597 cm^{-1} ; see Fig. 4 and related comments) [21,22]. These bands appear downshifted with respect to the positions they exhibit for neat liquid 3-aminopropyltriethoxysilane (3370, 3300, and 3200 cm^{-1} , in order; spectra not reported for the sake of brevity). Such perturbation of the vibrational spectrum monitors the occurrence of an interaction with other species. As a counterpart, the broadband in the range 3400–2200 cm^{-1} can be attributed to silanol hydrogen bonded to amino groups, as observed in the case of the adsorption of butylamine on silica [23]. In such interaction the Si–OH acts as H donors and the $-\text{NH}_2$ as H acceptor, through the lone pair on the nitrogen atom, with a consequent downshift of the stretching modes of both silanols and amino groups. Both *intramolecular* (Fig. 3a) and *intermolecular* (Fig. 3b) Si–



Fig. 3. Possible (a) intramolecular and (b) intermolecular Si–OH...NH₂ bridges.

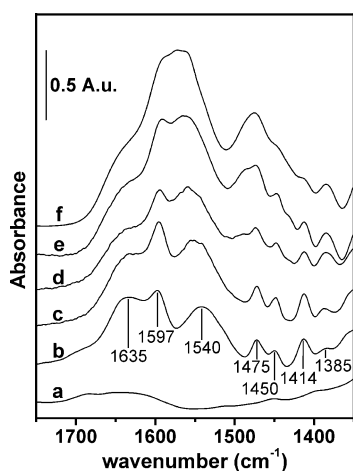


Fig. 4. Zoomed-in view of the 1750–1350 cm^{-1} region of the spectra of (a) the reference SiO_2 sample and (b) APS10, (c) APS20, (d) APS30, (e) APS40, and (f) APS50 catalysts, all outgassed at room temperature for 30 min.

OH...NH₂ bridges were envisaged in previous studies on silica areogels modified by aminoalkyl groups [24].

In spectra of catalysts with a progressively higher content of aminopropyl groups (Figs. 2c–f), only traces of the silanol band at 3610 cm^{-1} are present, while the components related to the stretching modes of $-\text{NH}_2$, $-\text{CH}_2-$, and $-\text{CH}_3$ groups appear more and more intense (methyl and methylene bands out of scale for APS40 and APS50, curves e and f). The ν_{asym} and ν_{sym} $-\text{NH}_2$ bands exhibit a progressive shift to lower frequencies, finally appearing at 3350 and 3284 cm^{-1} , respectively, in the spectrum of APS50 (Fig. 2f), indicating that they are due to $-\text{NH}_2$ groups experiencing a stronger hydrogen bonding with silanols. As a counterpart, the broadband in the range 3400–2200 cm^{-1} also exhibits a shift of the maximum to lower frequency.

Furthermore, other broad and ill-resolved components in the range 3150–3050 cm^{-1} are present. As commented on in more detail by discussing the bands in the region 1750–1350 cm^{-1} , where related absorptions are present, these components could be assigned to aminopropyl species constrained within the silica gel framework. A zoomed view of the spectra in the region 1750–1350 cm^{-1} is shown in Fig. 4.

With respect to the bare silica reference (Fig. 4a), the spectrum of the APS10 catalyst exhibits new components. The band at 1597 cm^{-1} is due to the deformation mode of $-\text{NH}_2$ groups, while those at 1475, 1450, and 1385 cm^{-1} can be ascribed to $\delta_{\text{asym}} -\text{CH}_3$, $\delta -\text{CH}_2$, and $\delta_{\text{sym}} -\text{CH}_3$, respectively, of methyl and methylene groups in the chain linking the $-\text{NH}_2$ groups to the silica surface. The position of the $\delta -\text{NH}_2$ band is almost coincident to that observed for neat liquid 3-aminopropyltriethoxysilane (not reported), in agreement with the lower sensitivity of this mode to the occurrence of weak hydrogen bonding between amino groups and silanols [23]. The remaining bands at 1635, 1540, and 1414 cm^{-1} correspond to the pattern of a $\text{R}'-\text{NH}_3^+-\text{OOC}-\text{R}''$ salt (R' and R'' being general alkyl chains), the component at 1414 cm^{-1} corresponding to the $\delta_{\text{sym}} \text{COO}^-$ mode and that at 1540 cm^{-1} to $\delta_{\text{sym}} \text{NH}_3^+$ vibrations, while the complex band at 1635 cm^{-1} results from superposition of the absorptions due to the $\delta_{\text{asym}} \text{COO}^-$ and $\delta_{\text{asym}} \text{NH}_3^+$ modes [20]. These species should be produced by reaction, during catalyst preparation and/or catalyst storage in air, of CO_2 present in air and two aminopropyl groups (PrNH_2) located on the silica matrix at sufficient distance to allow the formation of a $\text{PrNH}_3^+-\text{OOC}-\text{NHPr}$ adduct.

The bands due to these species are also present in the spectra of other APS materials (Figs. 4c–f), with an almost unchanged intensity, while they exhibit a $\delta -\text{NH}_2$ component at ca. 1595 cm^{-1} progressively more intense and slightly shifted to lower frequency as the content of aminopropyl groups increases, following the trend of the partner bands in the range 3300–3100 cm^{-1} (see Fig. 2 and related comments).

The spectra of these APS materials exhibit additional components, broader and complex, in the ranges 1580–1560 and 1500–1400 cm^{-1} , with a progressively higher inten-

sity as organic content increases. In particular, in the case of the APS50 catalyst the components in the range 1580–1560 cm^{-1} are so intense they appear as the dominant component (Fig. 4f).

As the occurrence of reactions involving amino groups, with the consequent formation of new species, is unlikely, these additional components could be assigned to aminopropyl species experiencing some peculiar interaction with their boundary. Taking into account that these components are particularly evident in the spectra of APS40 and APS50, which are characterized by a higher organic content and a lower specific surface area than APS10–APS30, it can be proposed that such interaction results from the constraints of aminopropyl species in the silica gel framework. The broadness and complexity of the bands due to such constrained species indicate the occurrence of some heterogeneity in the strength of this constraint.

It is difficult, at present, to discuss in detail the molecular effects involved in this interaction. For instance, the components in the range 1580–1560 cm^{-1} should correspond to the δ - NH_2 band of these constrained species, but their downshift appears too wide to be ascribed only to significantly stronger hydrogen bonding, and then additional factors should be considered. Calculations and molecular modeling are performed to clarify this point, and also allow a detailed assignment of other components in the range 1500–1400 cm^{-1} , which should correspond to methyl and methylene deformation bands of constrained aminopropyl and aminopropylethoxysilane species.

Of course, besides the absorption due to the deformation mode, the $-\text{NH}_2$ groups of the constrained aminopropyl groups should also exhibit the partner stretching bands. They could be recognized in the broad and complex features observed at high frequency in the range 3150–3050 cm^{-1} .

3.1.2.2. IR investigation of the interaction with benzaldehyde To obtain insights useful in rationalizing the catalytic behavior of the various materials, their interaction with benzaldehyde was monitored by IR.

Spectra in the range 1750–1350 cm^{-1} of the silica reference and on the catalysts before (dotted line) and after adsorption of benzaldehyde are compared in Fig. 5. In the case of the silica sample, only bands due to adsorbed benzaldehyde were observed (Fig. 5a). Their assignment is reported in Table 3. Benzaldehyde molecules are adsorbed on the silica surface via hydrogen bonding between the carbonyl group and surface silanols [25], and this results in a 10 cm^{-1} downshift of the carbonyl stretching (ν_{CO}) band, located at 1692 cm^{-1} , with respect to liquid benzaldehyde (1700 cm^{-1}), where only weaker forces between the molecules can occur.

An additional ν_{CO} component is present at 1700 cm^{-1} in the spectrum of benzaldehyde adsorbed on APS10 catalyst (Fig. 5b), likely due to benzaldehyde molecules in interaction, via weaker forces, with the aminopropyl chains. Such a component is the only ν_{CO} band observed in the spectra

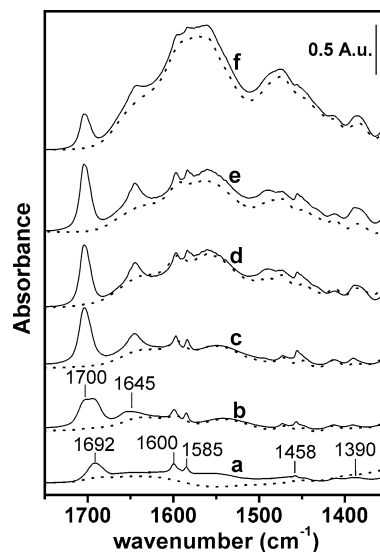


Fig. 5. IR spectra of benzaldehyde (full line) adsorbed (10 Torr, 1 h of contact) on (a) the reference SiO_2 and (b) APS10, (c) APS20, (d) APS30, (e) APS40, and (f) APS50 catalysts, all pre-outgassed at room temperature for 30 min. The spectra are compared with those of the samples before the admission of benzaldehyde (dotted curves).

Table 3

Assignment of the bands of adsorbed benzaldehyde, in the 1750–1350 cm^{-1} region, on the basis of Ref. [26]

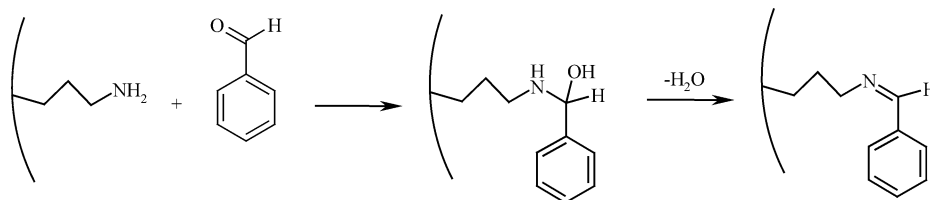
Assignment	Position (cm^{-1})
$\nu(\text{C}=\text{O})$	1692
$\nu(\text{C}=\text{C})$	1600
$\nu(\text{C}=\text{C})$	1585
$\nu(\text{C}=\text{C})$	1458
Rock (OC–H)	1390

of the other APS catalysts (Figs. 5c–f), indicating that no silanols are available for interaction with benzaldehyde. On the other hand, the spectra reported in Fig. 2 indicated that Si–OH interacting with the $-\text{NH}_2$ groups of aminopropyl chains are present. Comments on these features are reported later, taking into consideration also the data discussed in the following.

Furthermore, the intensity of the component at 1700 cm^{-1} , and of the related bands at lower frequencies, increases in the series APS10–APS40 (Figs. 5b–e) and then decreases for the APS50 (Fig. 5f), following a trend similar to that of the total pore volume of these materials (see Fig. 7).

In the case of APS catalysts, besides the bands due to adsorbed benzaldehyde an additional spectral pattern is present, characterized by a main component at 1645 cm^{-1} . This pattern can be assigned to imine species, the main component corresponding to the $\text{C}=\text{N}$ stretching mode [27]. Such species are the expected products of the reaction between the anchored aminopropyl groups and benzaldehyde molecules (Scheme 1).

After outgassing of benzaldehyde, only the pattern due to imine species is still present (Fig. 6, full lines). Interestingly,



Scheme 1.

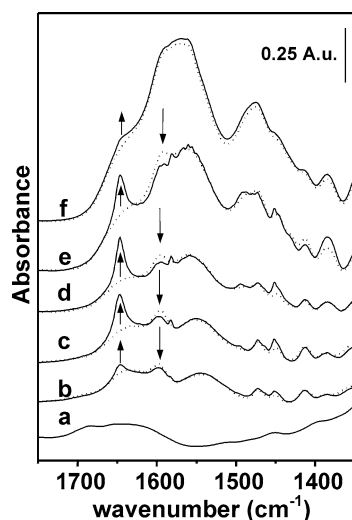


Fig. 6. IR spectra of samples (pre-outgassed at room temperature for 30 min) brought into contact for 1 h with benzaldehyde (10 Torr) and then outgassed for 30 min (full line): (a) reference SiO₂, and (b) APS10, (c) APS20, (d) APS30, (e) APS40, and (f) APS50 catalysts. The spectra are compared with those of the samples before the admission of benzaldehyde (dotted curves).

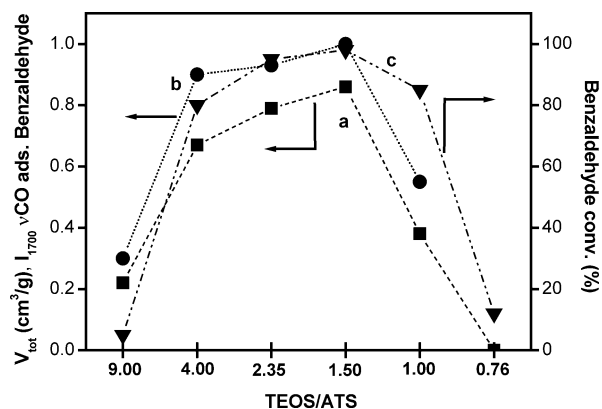


Fig. 7. Diagrams of (a) pore total volume (V_{tot} , cm³/g); (b) integrated relative intensity of the νCO mode at 1700 cm⁻¹ ($I_{1700} \nu\text{CO}$) (the values have been calculated assuming a value of 1 for $I_{1700} \nu\text{CO}$ for APS40); and (c) benzaldehyde conversion (%) for the series of APS catalysts.

removal of the components due to adsorbed benzaldehyde allows us to observe that the appearance of the imine bands is accompanied by a parallel erosion of a part the band at 1597 cm⁻¹ due to the deformation mode of -NH₂ groups in weak interaction with silanols (see Fig. 4 and related comments), as evidenced by comparison with the spectra of the catalysts before interaction with benzaldehyde (dotted lines).

These -NH₂ groups should then be the centers that reacted with benzaldehyde. Conversely, the δ -NH₂ components in the range 1580–1560 cm⁻¹ do not appear to be affected by the formation of imine. This feature agrees well with the supposed unaccessibility of the aminopropyl groups responsible for those components.

Finally, it can be noted that the amount of imine produced, proportional to the intensity of the C=N imine band, significantly increases from APS10 to APS20 (Figs. 6b and c), slightly increases from APS20 to APS40 (Figs. 6c–e), and then significantly decreases passing to APS50 (Fig. 6f), with a trend similar to that of the total pore volume of the catalysts (see Fig. 1).

We have previously examined the adsorption of benzaldehyde onto micelle templated aminopropylsilicas [28]. This study showed that benzaldehyde vapor reacts very rapidly (at 150 °C) with self-supporting wafers of micelle templated aminopropylsilica prepared by grafting of the silane onto presynthesized silica, and hardly reacts at all with materials prepared by direct co-condensation (at a 10 mol% aminopropyl content and at a 1:1 water:ethanol ratio), with a material produced in a more water-rich environment being intermediate in activity. This variation in the nucleophilicity of the amine groups was postulated as being due (partly) to the presence of a large number of ethoxy groups surrounding the amine group in the co-condensed systems, reducing their ability to interact with the aldehyde. The majority of these ethoxy groups are introduced during template extraction and, thus, may be situated predominantly close to the amine groups. While the nature of the materials is different here, due to significant differences in the methodologies for their preparation, their behavior appears to be analogous, with a relatively small number of alkoxy groups, perhaps more randomly distributed, correlating with reactive amine groups.

3.2. Catalytic activity

Table 4 compares the conversion of benzaldehyde (**1**) and the selectivity toward (*E*)-nitrostyrene (**3**) in the model reaction with nitromethane (**2**) (see Scheme 2) over the various catalysts after 2 h. The amount of catalyst used in each experiment was determined on the basis of the loading value to introduce the same supported propylamine equivalents (molar ratio benzaldehyde/propylamine = 40.0).

The efficiency of the catalysts was measured as conversion of benzaldehyde **1** and yield of (*E*)-nitrostyrene **3** per

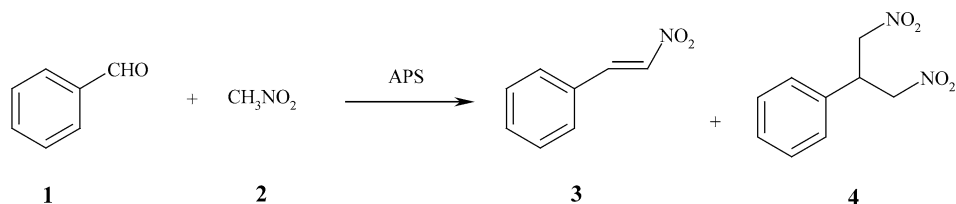


Table 4
(*E*)-Nitrostyrene synthesis catalyzed by different aminopropyl-based catalysts

Catalyst	Nitrogen content (%)	Loading (mmol/g)	1 Conversion (%)	3 Yield (selectivity) (%)	4 Yield (%)
APS10	1.99	1.42	5	5 (100)	–
APS20	3.64	2.60	80	75 (94)	4
APS30	4.84	3.46	95	90 (95)	5
APS40	5.68	4.06	98	95 (97)	3
APS50	6.27	4.48	85	80 (94)	5
APS60	7.48	5.34	12	10 (83)	2

cycle. We did not consider TON values since the number of catalytic sites taking effective part in the reaction was unknown. In fact, in these materials prepared by sol–gel technique it is expected that variable amounts of the propylamine are incorporated within the siliceous framework and it appears that their propylamine content, as measured by elemental analysis, does not necessarily correspond to the same equivalent of catalytically active base, since access to the catalytically active sites could be reduced or even hampered by the shape of the solid matrix. This is probably due to the formation of “pseudomicelles” of 3-aminopropyltriethoxysilane, during the catalyst preparation, that can originate a sort of island of aminopropyl groups interacting with each other and making the basic sites less accessible.

The mass balance was found to be within 2%. The (*E*)-stereochemistry of compound **3** was determined by ¹H NMR. In all cases compound **3** was the sole nitrostyrene isomer detected, accompanied by variable amounts of the dinitro compound **4** (Scheme 2). The selectivity with respect to compound **3** was high in all experiments, with only a small fraction of **3** undergoing subsequent nitro-Michael reaction to 2-phenyl-1,3-dinitropropane **4** (maximum value 5%). Conversion of **1** increases with the amount of propylamine incorporated into the catalyst and reaches the maximum value (98%) with APS-40. Then both conversion of **1** and selectivity of product **3** drop quickly, with catalysts APS-50 and APS-60 incorporating larger amounts of propylamine.

To obtain some insight into the relationships between the surface structure of the catalysts and their activity, the trends of V_{tot} , the conversion of benzaldehyde, and the integrated relative intensity of the νCO mode at 1700 cm^{-1} ($I_{1700}\ \nu\text{CO}$) due to benzaldehyde adsorbed on amino groups along the series of APS materials were compared (Fig. 7).

Table 5
Synthesis of variously substituted (*E*)-nitrostyrenes

Entry	R	R'	<i>t</i> (h)	<i>T</i> (°C)	Product 3	3 Yield (selectivity) (%)
1	H	H	2	90	3ax	95 (97)
2	OMe	H	2	90	3bx	89 (95)
3	OH	H	2	90	3cx	87 (94)
4	Cl	H	2	110	3dx^a	49 (96)
5	NO ₂	H	2	110	3ex^a	23 (95)
6	H	CH ₃	5	110	3ay^b	97 (98)
7	OMe	CH ₃	5	110	3by^b	92 (97)
8	OH	CH ₃	5	110	3cy^b	95 (96)

^a 110 °C.

^b Double amount of catalyst, 110 °C, 5 h.

It is worth noting that all three parameters follow a volcano trend, but with some interesting differences. The three parameters seem more strictly related to the APS10–APS40 series, suggesting that the sites able to adsorb benzaldehyde (under the IR experimental conditions) and convert it (in the reaction conditions) are located mainly in the porosity of these materials. On the other hand, the conversion of benzaldehyde decreases much less going from APS40 to APS50 than V_{tot} and $I_{1700}\ \nu\text{CO}$, and this could be related to some higher specific activity of the accessible active centers present in the APS50 catalyst.

The reaction was extended to different aldehydes and to nitroethane (Table 5). As nitroethane is less reactive than nitromethane, different reaction conditions were used to reach excellent yields, namely, double amount of catalyst and heating at 110 °C for 5 h. In all cases only (*E*)-nitrostyrenes were selectively obtained.

It is noteworthy that aldehydes bearing electron-withdrawing substituents are less reactive than electron-rich aldehydes. These results suggest that the reaction mechanism could be different from the classic nitroaldol pathway involving nitroalcohol formation followed by the dehydration step. In the present reaction we could hypothesize the initial formation of imine (as evidenced in IR spectra), which reacts with nitromethane to give the nitroamine adduct, as we already proposed [13]. The subsequent β -elimination affording the nitrostyrene product is favored by electron-withdrawing substituents on the aromatic ring. Therefore,

the rate-determining step could be the β -elimination step, which regenerates the amino function on the catalyst.

3.3. Leaching test and recycling

To exclude the possible leaching of any active catalytic species into solution, the model reaction between benzaldehyde and nitromethane was examined by following the standard procedure suggested by Lempers and Sheldon [29]. Thus, the reaction mixture was filtered at 90 °C after 30 min (when product **3a** was produced in 60% yield) and the filtrate was further heated at 90 °C for 2 h. Product **3a** was detected in 65% total yield (60% + 5%). In contrast, addition of both benzaldehyde (5 mmol, 0.53 g) and nitromethane (6 mL) to the recovered solid catalyst and heating at 90 °C for 2 h afforded nitrostyrene **3a** in 90% yield. These results confirm that the reaction actually occurs on the supported propylamine.

The recycling of the APS-40 catalyst was conducted by filtering, washing with methylene chloride, drying at 90 °C for 2 h (under vacuum), and immediately reusing without any activation. On reuse, the catalyst suffered some deactivation giving compound **3ax** in 95, 90, 60, and 25% yields in four cycles.

To understand the catalyst deactivation we reacted benzaldehyde with nitromethane over APS-40 in the presence of an equimolecular amount of nitrostyrene. Product **3ax** was obtained in 80% yield after 5 h under these conditions, suggesting that the catalyst is still active, but at a lower reaction rate. Moreover, IR investigation of the reused catalyst indicated the presence of strong bands at 1635, 1540, and 1414 cm^{-1} corresponding to the pattern of $\text{R}'-\text{NH}_3^+-\text{OOCR}''$ salt, probably due to reaction of the supported propylamine with CO_2 present in the air, or with some benzoic acid present in the benzaldehyde or produced by in situ oxidation, the reaction not being performed in a controlled atmosphere.

To regenerate the propylamine active sites, the reused catalyst was treated with a 10% ethanolic solution of propylamine and then washed with ethanol in a Soxhlet apparatus for 4 h. After being dried at 110 °C for 2 h the catalyst was tested in the model reaction affording product **3ax** in 78% yield and finally showing that most of the active sites could be regenerated by convenient basic treatment.

4. Conclusions

The catalytic activity of the different APS materials prepared by sol–gel technique depends on the physicochemical properties of the solids which are conveniently tuned by changing the relative ratio of the starting sol components TEOS/ATS. Studies of the textural and adsorption properties of the APS materials indicated that increasing the amine percentage over 40% in the gel synthesis causes a collapse of the surface area and pore volume of the solids, with con-

finement of the amine groups in inaccessible environments. The reactivity results exhibit a similar trend.

With the best catalyst, APS-40, (*E*)-nitrostyrene was thus obtained in high yield (95%) and selectivity (97%) under mild heterogeneous conditions. The reaction was extended to nitroethane and to different aldehydes, suggesting a peculiar reaction mechanism.

Acknowledgments

The authors acknowledge the support of the Ministero dell'Università e della Ricerca Scientifica e Tecnologica (MURST), Italy, the Consiglio Nazionale delle Ricerche (CNR), Italy, and the University of Parma (National Project "Processi Puliti per la Chimica Fine"). D.J.M. thanks the Royal Society for a University Research Fellowship.

The authors are grateful to the Centro Interdipartimentale Misure (CIM) for the use of NMR and mass instruments and to Mr. Pier Antonio Bonaldi (Lillo) for technical collaboration.

Finally, authors at the Dipartimento di Chimica Organica e Industriale of Parma and at the Dipartimento di Chimica IFM of Torino participated in this work within the framework of the activity of the Interuniversity Consortium "Chemistry for the Environment"—INCA.

References

- [1] A.R. Sheldon, *Chem. Ind. (London)* (1997) 12.
- [2] C. Adams, *Chem. Ind. (London)* (1999) 740.
- [3] J.H. Clark, D.J. Macquarrie, *Chem. Soc. Rev.* (1996) 303.
- [4] G. Rosini, in: B.M. Trost, I. Fleming, C.H. Heathcock (Eds.), *Comprehensive Organic Synthesis*, Pergamon, Oxford, 1991, p. 321.
- [5] R. Ballini, G. Bosica, *J. Org. Chem.* 62 (1997) 425.
- [6] R. Ballini, G. Bosica, P. Forconi, *Tetrahedron* 52 (1996) 1677.
- [7] R. Ballini, F. Bigi, E. Gogni, R. Maggi, G. Sartori, *J. Catal.* 191 (2000) 348.
- [8] G. Sartori, F. Bigi, R. Maggi, A. Mazzacani, G. Oppici, *Eur. J. Org. Chem.* (2001) 2513.
- [9] S. Carloni, D.E. De Vos, P.A. Jacobs, R. Maggi, G. Sartori, R. Sartorio, *J. Catal.* 205 (2002) 199.
- [10] G. Sartori, A. Armstrong, R. Maggi, A. Mazzacani, R. Sartorio, F. Bigi, B. Dominguez-Fernandez, *J. Org. Chem.* 68 (2003) 3232.
- [11] D.J. Macquarrie, R. Maggi, A. Mazzacani, G. Sartori, R. Sartorio, *Appl. Catal. A* 246 (2003) 183.
- [12] V.J. Bulbule, V.H. Deshpande, S. Velu, A. Sudalai, S. Sivasankar, V.T. Sathe, *Tetrahedron* 55 (1999) 9325.
- [13] G. Demicheli, R. Maggi, A. Mazzacani, P. Righi, G. Sartori, F. Bigi, *Tetrahedron Lett.* 42 (2001) 2401.
- [14] M. Lakshmi Kantam, P. Streekanth, *Catal. Lett.* 57 (1999) 227.
- [15] L.L. Hench, J.K. West, *Chem. Rev.* 90 (1990) 33.
- [16] E.I. Ko, in: G. Erdtl, H. Knozinger, J. Weitkamp (Eds.), *Handbook of Heterogeneous Catalysis*, Pergamon, Oxford, 1997, p. 321.
- [17] P.A. Webb, C. Orr, *Analytical Methods in Fine Particle Technology*, Micromeritics Instruments Corporation, Norcross, USA, 1997.
- [18] F. Roquerol, J. Roquerol, K. Sing, *Adsorption by Powders and Porous Solids*, Academic Press, UK, 1999.
- [19] A. Burneau, J.P. Gallas, in: A.P. Legrand (Ed.), *The Surface Properties of Silicas*, Wiley, Chichester, 1998, p. 147.
- [20] N.B. Colthup, L.H. Daly, S.E. Wiberley, *Introduction to Infrared and Raman Spectroscopy*, 2nd ed., Academic Press, New York, 1975.

- [21] J.J.C. Teixeira-Dias, L.A.E. Batista de Carvalho, A.M. Amorim da Costa, I.M.S. Lampreia, E.F.G. Barbosa, *Spectrochim. Acta, Part A* 42 (1986) 589.
- [22] N. Sato, Y. Hamada, M. Tsuboi, *Spectrochim. Acta, Part A* 43 (1987) 943.
- [23] G. Ramis, G. Busca, *J. Mol. Struct.* 193 (1989) 93.
- [24] N. Hüsing, U. Schubert, R. Mezei, P. Fratzl, B. Riegel, W. Kiefer, D. Kohler, W. Mader, *Chem. Mater.* 11 (1999) 451, and references therein.
- [25] M. Allian, E. Borello, P. Ugliengo, G. Spanò, E. Garrone, *Langmuir* 11 (1995) 4811.
- [26] H.A. Szymanski, *Interpreted Spectra*, vol. 1, Plenum, New York, 1964, p. 83.
- [27] J. Fabian, M. Legrand, P. Poirier, *Bull. Soc. Chim. Fr.* 23 (1956) 1499.
- [28] D. Brunel, A.C. Blanc, E. Garrone, B. Onida, M. Rocchia, J.B. Nagy, D.J. Macquarrie, *Stud. Surf. Sci. Catal.* 142 (2002) 1395.
- [29] H.E.B. Lempers, R.A. Sheldon, *J. Catal.* 175 (1988) 62.